NASA Technical Memorandum 83438

Aerodynamic Performance of a Fan Stage Utilizing Variable Inlet Guide Vanes (VIGVs) for Thrust Modulation

Richard R. Woollett
Lewis Research Center
Cleveland, Ohio

Prepared for the
Nineteenth Joint Propulsion Conference
cosponsored by the AIAA, SAE, and ASME
Seattle, Washington, June 27-29, 1983

NASA

AERODYNAMIC PERFORMANCE OF A FAN STAGE UTILIZING VARIABLE INLET GUIDE VANES (VIGVs) FOR THRUST MODULATION

Richard R. Woollett
National Aeronautics and Space Administration
Lewis Research Center
Cleveland, Ohio

Abstract

An experimental research program was conducted in the Lewis Research Center's 9x15-foot (2.74x4.57 m) Low Speed Wind Tunnel to evaluate the aerodynamic performance of an inlet and fan system with variable inlet guide vanes (VIGVs) for use on a subsonic V/STOL aircraft. At high VIGV blade angles (lower weight flow and thrust levels), the fan stage was stalled over a major portion of its radius. In spite of the stall, fan blade stresses only exceeded the limits at the most extreme flow conditions. It was found that inlet flow separation does not necessarily lead to poor inlet performance or adverse fan operating conditions. Generally speaking, separated inlet flow did not adversely affect the fan blade stress levels. There were some cases, however, at high VIGV angles and high inlet angles-of-attack where excessive blade stress levels were encountered. An evaluation term made up of the product of the distortion parameter, K_θ, the weight flow and the fan pressure ratio minus one, was found to correlate quite well with the observed blade stress results.

Symbols

ET	evaluation term, $K_\theta \times W \times (PR - 1)$
K_θ	distortion parameter, ref. 5
P_2/P_0	inlet total pressure recovery, ratio of average total pressure to free stream total pressure
P_3/P_2	fan total pressure ratio, ratio of total pressure at stator exit to average total pressure at the inlet diffuser exit plane
PR	average total pressure ratio across fan stage and VGIVs
Pt	total pressure tube
S_1	flow separation criterion at the diffuser exit when the total pressure measured 0.0063 y/H units off the duct wall is equal to the local static pressure
S_4	flow separation criterion at the diffuser exit when the total pressure measured measured 0.064 y/H units off the duct wall is equal to the local static pressure
V_{th}/V_0	inlet velocity ratio, ratio of average inlet throat velocity to the free-stream velocity
W	inlet (fan) weight flow, kg/sec (lbs/sec)
y/H	non-dimensional height, ratio of the height of the total pressure probe from the duct wall to the height of the flow passage
α	inlet angle-of-attack, deg
β	VIGV blade deflection angle, deg

Subscript:

r	rotor
s	stator
sep	separation

Introduction

Developing an advanced subsonic vertical or short takeoff landing (V/STOL) aircraft requires the solutions to some of the most challenging and complex propulsion problems that confront the aircraft industry today. The propulsion system, i.e., the engine, nacelle and controls is required to operate over a wide range of conditions during flight through the vertical takeoff and landing corridor. In particular, during the approach to landing, the engine nominal thrust may vary from 50 to 100 percent of design thrust. For the necessary control requirements during the approach, an additional variation of ±25 percent about the nominal thrust may be required. Hence, the overall range of thrust variance required can be as high as from 25 to 125 percent of the design value. For the tilt-nacelle type of subsonic V/STOL aircraft, illustrated in figure 1, the propulsion system inlet must be designed to provide high quality air flow to the engine in order to maintain high thrust levels and also avoid excessive fan or compressor blade stress levels. This high quality airflow must be provided at all conditions in the flight envelope, including the approach to landing where the inlet angle-of-attack ranges from 0 degrees to as high as 120 degrees. Hence, for the tilt-nacelle subsonic V/STOL aircraft, the propulsion system is required to provide thrust variations from 25 to 125 percent of design while operating at rather severe values of inlet angle of attack.

As was shown in reference 1, variable inlet guide vanes (VIGVs) are an effective means for providing this needed thrust modulation, and in fact can provide it while the fan is running at a constant and high value of fan rotational speed. This has the advantage of permitting thrust changes to occur quickly, which is another necessary requirement for effective aircraft control. It was also shown (ref. 1) that the required levels of thrust modulation could be obtained with VIGVs, even at combinations of freestream velocity and angle-of-attack where the inlet internal flow was separated.

The purpose of this paper is to explore the criteria used to define inlet flow separation, and also to examine the performance of the VIGV/fan stage including operation with inlet flow separation.

Experimental Model

The results presented in this paper were obtained in an experimental research program designed to investigate the aerodynamic performance of a relatively thick-lipped inlet for a tilt-nacelle V/STOL aircraft. The performance of several different methods for attaining thrust modulation was also determined including the use of VIGVs. Preliminary results of the program were reported in reference 1.

The research program was conducted in the NASA Lewis Research Center's 9x15 foot (2.74x4.57 m) Low

Speed Wind Tunnel, an atmospheric tunnel. A complete description of the tunnel and its aerodynamic characteristics are contained in reference 2. The fan model installed in the test section of the tunnel is shown in figure 2. The model fan is 0.508 meter in diameter and represents an approximately 0.3 scale model for a twin engine 18 000 kg (40 000 pound) gross weight airplane. The fan has 15 blades, a hub to tip ratio of 0.46 and a design tip speed of 2.3 m/sec (700 ft/sec). At its design speed of 8020 rpm the fan pressure ratio is 1.17. The fan may be operated to a speed of 120 percent with a pressure ratio of 1.25. The model is supported by a horizontal strut and a vertical pipe stand and is rotated in the horizontal plane for angle-of-attack variation.

The inlet shown schematically in figure 3(a) was 0.6 fan diameters in length and had a lower lip area contraction ratio (highlight area/throat area) of 1.69. The inlet was instrumented internally with static pressure taps and inlet overall performance (total pressure recovery and distortion) was measured at the diffuser exit plane with six equally spaced radial rakes. As indicated in figure 3(b), the 1st and 4th total pressure probes (counting from the outer wall) of the bottom or windward rake, served as flow separation indicators during the tests. Further details on this method for detecting inlet flow separation can be found in reference 3.

The VIGV stage shown in figure 3(a) was made up of 20 full span vanes of NASA 63-009 series profile. The front portion of each vane is fixed and only the rear portion is rotated. A photograph of the VIGV stage and its actuation mechanism is shown in figure 4. Four circumferential rakes, which were positioned behind the VIGVs at roughly 0 degrees, 90 degrees, 180 degrees and 270 degrees, measured the flow angle downstream of the VIGVs. These rakes each had three 3-tube directional probes located on a 22.9 cm (9") radial arc measured from the centerline of the fan.

At the fan stator exit, a 5 spoke total pressure rake was installed, as shown in figure 3(a). Each spoke had 10 total pressure tubes and either one or two total temperature probes. In addition, 5 centerbody and 5 casing static pressures were measured at the stator exit rake station. Fan pressure and temperature rise across the fan stage and fan exit distortion parameters were calculated using this instrumentation. The fan duct exited into the tunnel through a fixed area convergent nozzle. Static pressures were measured in the exit duct and at the nozzle exit.

Fan blade stress levels were also measured at all conditions tested. Details of the methods for obtaining the blade stress data are given in reference 4.

Results and Discussion

As indicated in the introductory remarks, there are two major topics to be discussed in this paper. The first is the criterion used to establish inlet flow separation, and more specifically, the criterion that is most important in terms of adequate fan operation. The second topic is the performance of the fan with VIGVs including operation with separated inlet flow.

Inlet Flow Separation Criteria

We have seen in a previous report (ref. 1) that the required levels of thrust modulation could be obtained with VIGVs even at combinations of freestream velocity and angle-of-attack where the inlet internal flow was separated. These results are repeated from the reference in figure 5 where we have plotted a calculated gross thrust as a function of the VIGV deflection angle, β. When β is zero the VIGVs are aligned with the axis of the fan. The bar on the ordinate indicates the required thrust variation for V/STOL operation. Data for angles-of-attack of zero and 90 degrees are both presented on the figure. At an angle of attack of 0 degrees, the figure indicates that the full range of required thrust variation can be obtained by varying the VIGV blade angle from 0 degrees to 40 degrees. At an angle-of-attack of 90 degrees, two points need to be made concerning the results. First, the inlet flow is separated over the full range in VIGV blade angle and secondly, the maximum attainable VIGV blade angle was only 30 degrees. Excessive blade stresses prevented operation at a VIGV angle of 40 degrees. As indicated, in spite of the inlet flow separation, thrust variation comparable to that obtained at a 0 degree angle-of-attack could be obtained up to the 30 degree VIGV angle. The restricted VIGV operating range at a 90 degree angle-of-attack, however, resulted in about a 40 percent reduction in the range of thrust variation required for V/STOL operation. A more detailed examination of these results is warranted.

Figure 6 indicates the angle-of-attack where inlet flow separation occurs as a function of VIGV blade angle and hence also inlet weight flow. Shown on the figure is the inlet angle-of-attack and weight flow requirement for the tilt-nacelle V/STOL concept at this freestream velocity. Three different performance curves are noted. The lowest curve, S_1, is the inlet flow separation bound indicated when the first total pressure tube at the fan face (closest to the outer wall) is used as the separation criterion (fig. 3(b)). The middle curve, S_4, is the separation bound indicated when the fourth tube is used as the separation criterion. The upper curve is the angle-of-attack bound at which fan blade stresses reached the maximum safe value. The upper curve is obtained by observing the blade stress for a fan speed sweep from 20 percent to 110 percent of design speed for each value of VIGV deflection angle. The way to interpret this upper curve is that, at angles-of-attack below the curve, the fan can be operated at any rotational speed with the fan blade stresses below the safe limit. At angles-of-attack above the curve, there is some rotational speed between 20 and 110 percent of design where the safe limit will be exceeded.

It is obvious from the figure that whether or not the inlet is considered to be compatible with the fan is highly dependent on the separation or evaluation criterion used. If one uses the S_1 separation criterion (as was done for the results presented in fig. 5) then the inlet and fan will be determined not to be compatible because over roughly 33 percent of the fan operating range, the inlet flow will be separated according to that criterion and the thrust variation range will be reduced by about the same percentage. If the S_4 separation criterion or the blade stress criterion

are used, then with the exception of a small region at the low weight flows for the S_4 criterion, the fan and inlet would be compatible. The appropriate compatibility criterion must be selected based on other factors such as inlet total pressure recovery and distortion at these conditions, and the sensitivity of the particular fan design to these parameters.

Figure 7 shows inlet total pressure recovery as a function of VIGV blade angle and weight flow at the same freestream velocity of 30.9 m/sec (60 knots) and at 90 degrees inlet angle-of-attack. Note that although the S_1 indicator shows separated flow over the full range in VIGV blade angles and S_4 shows separated flow over a small portion of the curve, the recovery levels are quite high (greater than about 99 percent). Hence, in terms of inlet total pressure recovery (and ultimately propulsion system thrust), separation as determined by either S_1 or S_4 has, in this case, little effect.

Figure 8 shows the inlet total pressure distortion parameter, K_θ, (see ref. 5) plotted against the ratio of inlet throat velocity to freestream velocity. This ratio is one that is commonly used to present inlet separation data (ref. 6). Data are shown for all inlet conditions tested (various combinations of freestream velocity, inlet weight flow, VIGV blade angle, and angle-of-attack) with different symbols used to indicate the type of separation present. The results indicate that when the inlet flow is attached, the value of K_θ generally remains below a value of 0.038. When the S_1 type of separation exists, K_θ is greater than or equal to 0.038. When the S_4 type of separation exists, K_θ is greater than or equal to 0.078. Hence, at least in this case, a simple measurment made by a total pressure tube located a specified distance off the fan casing can be used to establish the lower bound for a much more complicated distortion parameter.

The point of this discusstion is that the criterion used to determine whether or not a particular inlet design is compatible with a particular fan design must be carefully selected. In the specific example discussed here, selection of the separation parameter S_1 as the criterion for acceptable inlet/fan compatibility would not be correct. Even with this separation present, the fan blade stresses were acceptable, the inlet pressure recovery was high, and the distortion parameter, K_θ, was in the low range from 0.038 to 0.078. Selection of the separation parameter S_4 would also not be the proper inlet/fan compatability criterion since again the blade stresses are acceptable and recovery is high. The proper evaluation criterion for inlet/fan compatability would predict blade stress, or at least the maximum allowable blade stress, and may well be different for different combinations of inlet and fan design. The criterion would probably include at least a parameter relating to the level of inlet distortion and a parameter relating to the rotor loading.

Fan Performance

Examples of the inlet-fan system performance and interaction are depicted in figures 9 and 10. Figure 9 shows the change in the radial total pressure profiles at the stator exit when the VIGV deflection angle is increased from 0 to 40 degrees; the fan speed is 110 percent of design. The inlet is at zero degrees angle-of-attack with a freestream velocity of 20.6 m/sec (40 knots). As the VIGV deflection angle increases, the quality of the stator exit flow decreases until, at a VIGV angle of 40 degrees, a fairly large sector of the flow is at a pressure ratio of less than one, indicating flow separation or stall in either the rotor or stator. There is a sizeable amount of circumferential distortion present when β is not equal to 0 degrees even at alpha equals 0 degrees. The source of the distortion was not determined; however, a contributing factor could possibly be the low total pressure wakes from the VIGVs intercepting the total pressure probes of the stator exit rake. The values of inlet flow distortion, K_θ, are listed along with the fan weight flow and fan pressure ratio on each of the curves. As expected, at an inlet angle-of-attack of 0 degrees, the quality of the inlet flow is quite good (low K_θ). The blade stresses were low at all of the VIGV settings in spite of the apparent stall or flow separation in either the rotor or stator at the higher values of β.

Figure 10 shows the stator exit profiles for an inlet angle-of-attack of 90 degrees, where the inlet flow was separated according to criteria S_1 and S_4. A comparison of figures 9 and 10 shows little change in the stator exit profiles for particular settings of β. However, inlet performance was poorer as evidenced by the increased values of K_θ. As an example, for β = 30 degrees, the fan weight flow, pressure recovery, and stator exit total pressure profile were essentially unaffected by increasing the inlet angle-ofattack to 90 degrees. However, K_θ increased from 0.0925 to 0.086. Blade stress levels increased with increasing K_θ so as to actually prevent taking data at β = 40 degrees. In general, whenever both weight flow and inlet distortion were high, blade stress was unacceptable. As the weight flow was decreased, by increasing VIGV blade angle, K_θ increased due to the increasing severity of the flow conditions in the inlet. For the conditions of figure 10, K_θ is increasing at a faster rate than the weight flow decreases, resulting in high blade stress for β = 30 degrees. This relation is demonstrated by the plot in figure 11 where the percentage of maximum allowable blade stress is plotted as a function of the parameter $IT = (K_\theta) \times (W) \times (PR - 1)$. The parameter IT is made up of terms that relate to the degree of inlet distortion (K_θ) and the degree of fan blade loading (W and PR - 1). The blade stress limit is reached when IT is approximately 0.95. For the data points shown in figure 11, K_θ varied from 0.0189 to 0.1245, a factor of 6.6; W varied from 32.7 to 66.2, a factor of 2; and (PR - 1) varied from 0.023 to 0.231, a factor of 10. None of the variables by themselves could collapse the data as well as IT. Some of the scatter in the data could be explained by the fact that the blade stress data was neither taken at exactly the same time or at exactly the same fan speed as the aerodynamic data. As an example, the resonate blade stress measurements were taken at 8070 and 6010 rpm while the pressure measurements were taken at roughly 8900 and 5700 rpm.

To summarize, increasing VIGV blade angle with the inlet at an angle-of-attack of 0 degrees (low inlet distortion parameter K_θ) results in

an eventual stall of the fan stage over some radial extent. This still did not result in excessive blade stresses. However, when the inlet angle-of-attack was increased to 90 degrees, blade stress limits were reached for values of β in excess of approximately 30 degrees. Fan stage performance, as measured by weight flow and pressure rise, was not substantially changed due to operation at high angle-of-attack.

From the VIGV, rotor and stator blade angles, the inlet mass flow and the rotor rotational speed, the flow angle-of-attack into both the rotor and stator blades can be calculated as a function of radial location. Such first-order calculations were made neglecting compressibility, viscous, and 3-dimensional effects, to develop an understanding of what was actually occurring through the fan stage. It is recognized that these calculations are in no way precise, but they do provide some qualitative insight.

The calculated angle-of-attack between the local flow and the rotor and stator chord lines is presented in figure 12. The total change in angle-of-attack along the span of the rotor blade varies from +1. to -2.5 degrees and along the span of the stator vane from -2. degrees to -10. degrees. This suggests that the flow should be well behaved through the fan stage. This conclusion is supported by the stator exit total pressure profiles of figure 9(a). Rotor and stator leading edge angle-of-attack for the case of a VIGV blade setting of 40 degrees at a fan speed of 110 percent are presented in figure 13. It can be seen that the angle-of-attack of the rotor varies from -15 degrees at the hub to +5 degrees at its tip. This suggests that the flow would most likely separate in the rotor near the hub. If we assume the flow somehow does not separate off the rotor, then the angle-of-attack that the leading edge of the stator experiences changes from 11 degrees to 20 degrees as the measuring station varies from the hub to the tip. From these first order calculations, it is evident that blade stall should exist in the fan stage. The stator exit rake data of figure 9(c) supports this conculsion by indicating low total pressure at both the hub and tip.

There is an added complication that will mollify the angle-of-attack calculations somewhat. The VIGVs did not turn the flow the same angle as the geometric setting of the VIGVs, i.e., β. This is shown in figure 14 where we can see that when the VIGVs are set at 40 degrees, the effective turning angle that the flow experiences is roughly 31 degrees. The effective angle setting of the VIGVs presented in figure 13 will reduce the calculated angles-of-attack at the rotor that are presented in figure 13.

It should be remembered that all of the results presented in this paper in terms of inlet and fan operation and interaction are specific to the particular inlet and fan designs involved in this test program. Effects of inlet distortion or fan performance, particularly in terms of fan blade stress levels, would be expected to be significantly different for other fan and/or inlet designs. Nevertheless, the results point out the nature of the fan/ nacelle design problems for subsonic V/STOL aircraft, and indicate the considerations that the propulsion system designer must take into account.

Conclusions

An experimental research program was conducted in the Lewis Research Center's 9x15-foot (2.74x4.57 m) Low Speed Wind Tunnel to evaluate the aerodynamic performance of an inlet and fan system with variable inlet guide vanes (VIGVs) for use on a subsonic V/STOL aircraft. Major results of the program are summarized as follows:

1. The particular criterion used to evaluate inlet performance in terms of internal flow separation must be carefully selected. It was shown that inlet flow separation, as detected by instrumentation located close to the inlet surface at the diffuser exit plane, does not necessarily lead to poor inlet performance or adverse fan operating conditions (at least for the fan used in this program).

2. At high VIGV blade angles (lower weight flow and thrust levels), the fan stage was stalled over a major portion of its radius. This stall was shown to be a result of high blade angles-of-attack into the rotor and/or stator. In spite of the stall, however, fan blade stresses only exceeded the limits at the most extreme flow conditions.

3. Generally speaking, separated inlet flow did not adversely affect the fan blade stress levels. There were some cases, however, at high VIGV angles and high inlet angles-of-attack where excessive blade stress levels were encountered.

4. An Evaluation Term made up of the product of the distortion parameter, $K\theta$, the weight flow and the fan pressure ratio minus one, was found to correlate the observed blade stress results.

References

1. Woollett, R. R., "Thrust Modulation Methods for a Subsonic V/STOL Aircraft," AIAA Paper 81-2633, Dec. 1981.
2. Yuska, J. A., Diedrich, J. H., and Clough, N., "Lewis 9x15 Foot V/STOL Wind Tunnel," NASA TM X-2305, July 1971.
3. Burley, R. R., "Effect of Lip and Centerbody Geometry on Aerodynamic Performance of Inlets for Tilting-Nacelle VTOL Aircraft," AIAA Paper 79-0381, Jan. 1979.
4. Williams, R. C., Diedrich, J. H. and Shaw, R. J., "Turbofan Blade Stresses Induced by the Flow Distortion of a VTOL Inlet at High Angles of Attack," NASA TM-82963, Jan. 1983.
5. Dicus, J. H., "Fortran Program to Generate Engine Inlet Flow Contour Maps and Distortion Parameters," NASA TM X-2967, Feb. 1974.
6. Boles, M. A., and Stockman, N. O., "Use of Experimental Separation Limits in the Theoretical Design of V/STOL Inlets," AIAA Paper 77-878, July 1977.

Figure 1. - Tilt-nacelle subsonic V/STOL landing sequence.

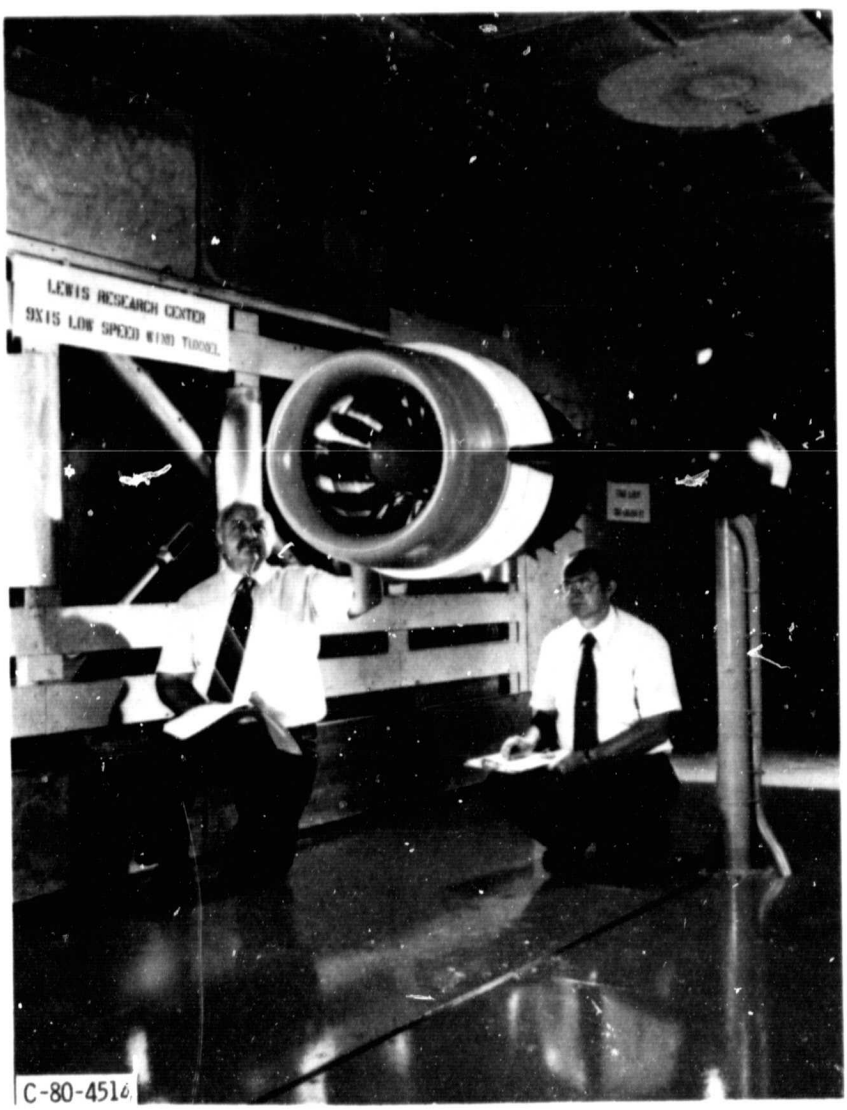

Figure 2. - Model installation in NASA LeRC low speed tunnel.

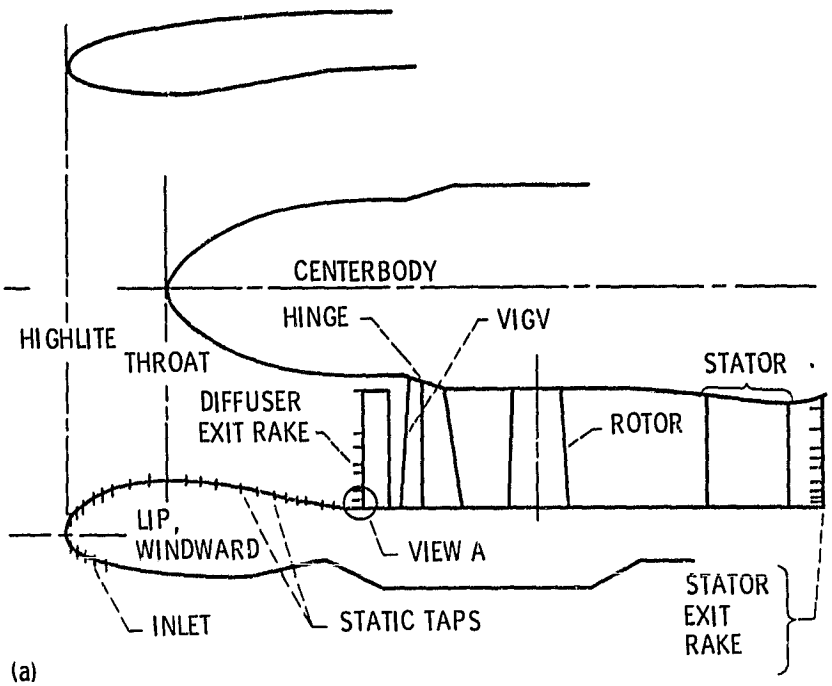

(a)

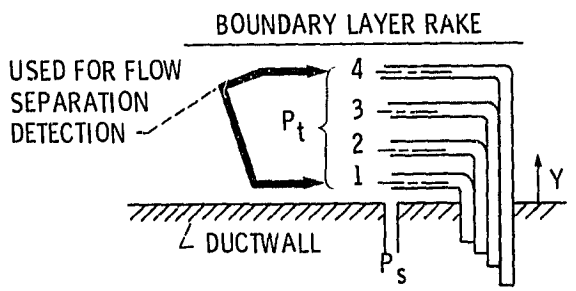

H = 5.404 in. (0.1373 m)

P_t	y/H
1	0.0063
2	.0192
3	.0414
4	.064

(b)

(a) Schematic of inlet/VIGV/fan assembly showing instrumentation.
(b) Instrumentation used for flow separation detection, view A.

Figure 3. - Details of inlet, VIGV, and fan assembly showing instrumentation.

Figure 4. - Photograph of VIGV subassembly.

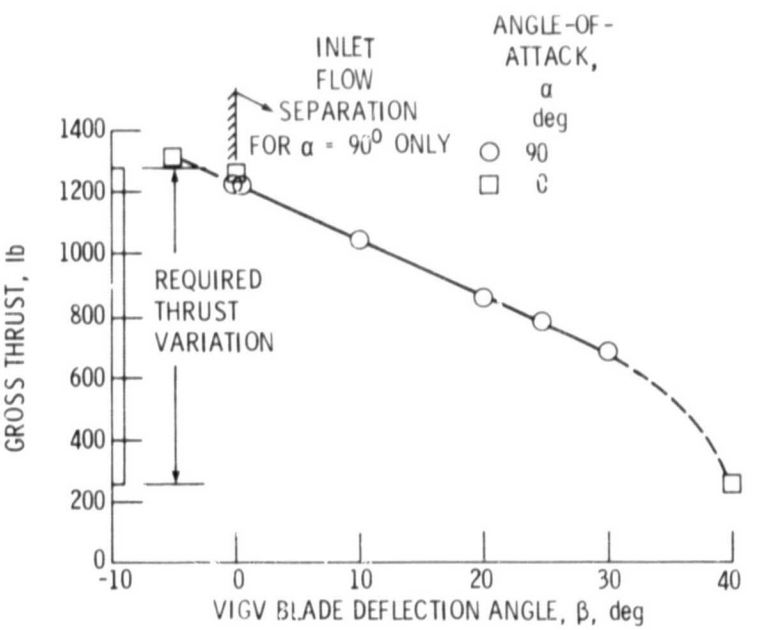

Figure 5. - Effect of inlet angle-of-attack on thrust variation for an inlet-VIGV-fan system. Fan speed, 110% of design; freestream velocity, 30.9 m/sec (60 knots).

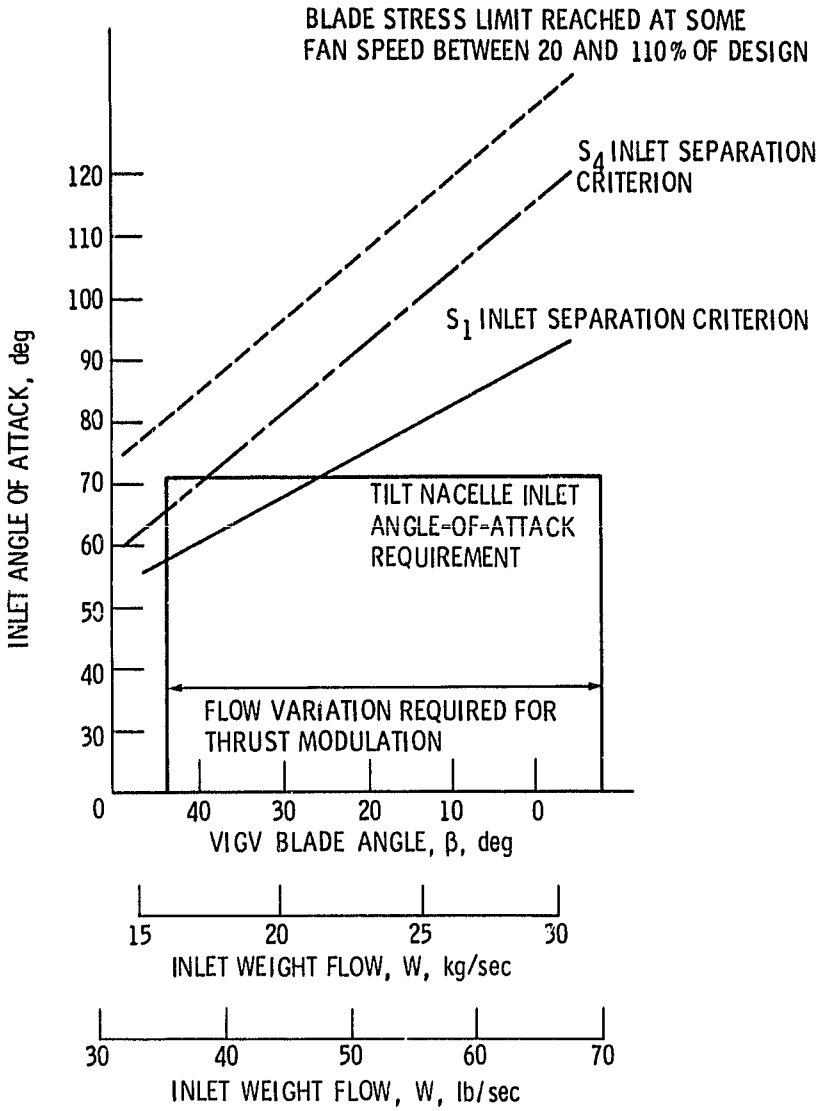

Figure 6. - Performance characteristics of an inlet with VIGV thrust modulation system. Free-stream velocity, 30.9 m/s (60 knots); fan speed, 110% design.

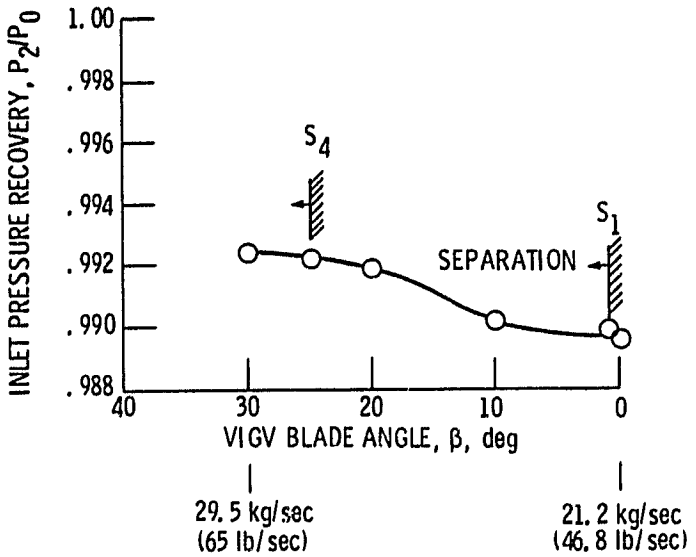

Figure 7. - Inlet total pressure recovery as a function of VIGV blade angle. Freestream velocity, 30.9 m/sec (60 knots); fan speed, 110% of design; inlet angle-of-attack, 90^0.

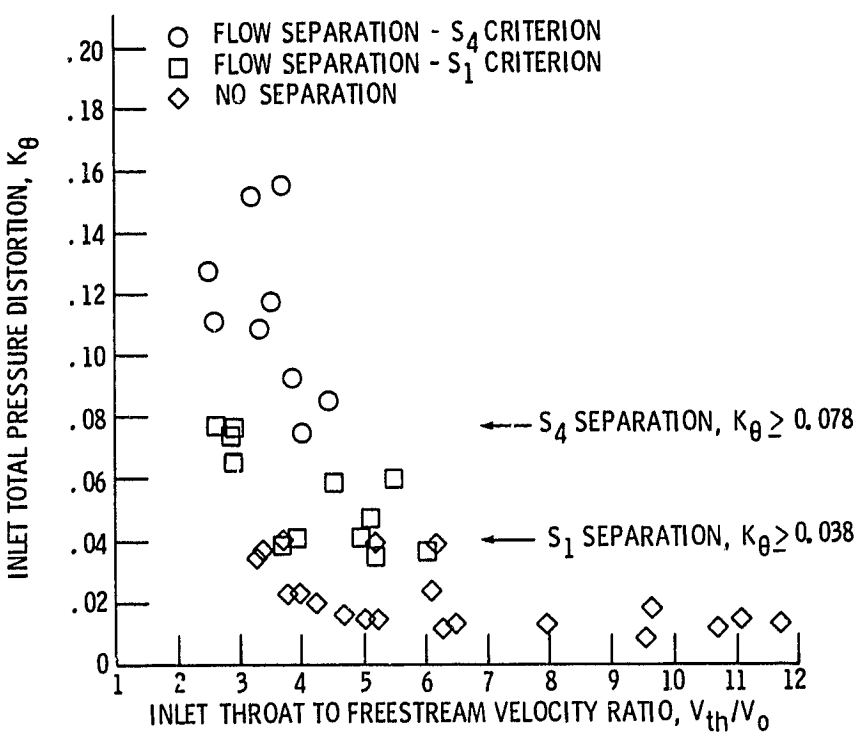

Figure 8. - Distortion parameter, K_θ, as a function of the ratio of inlet throat velocity to freestream velocity.

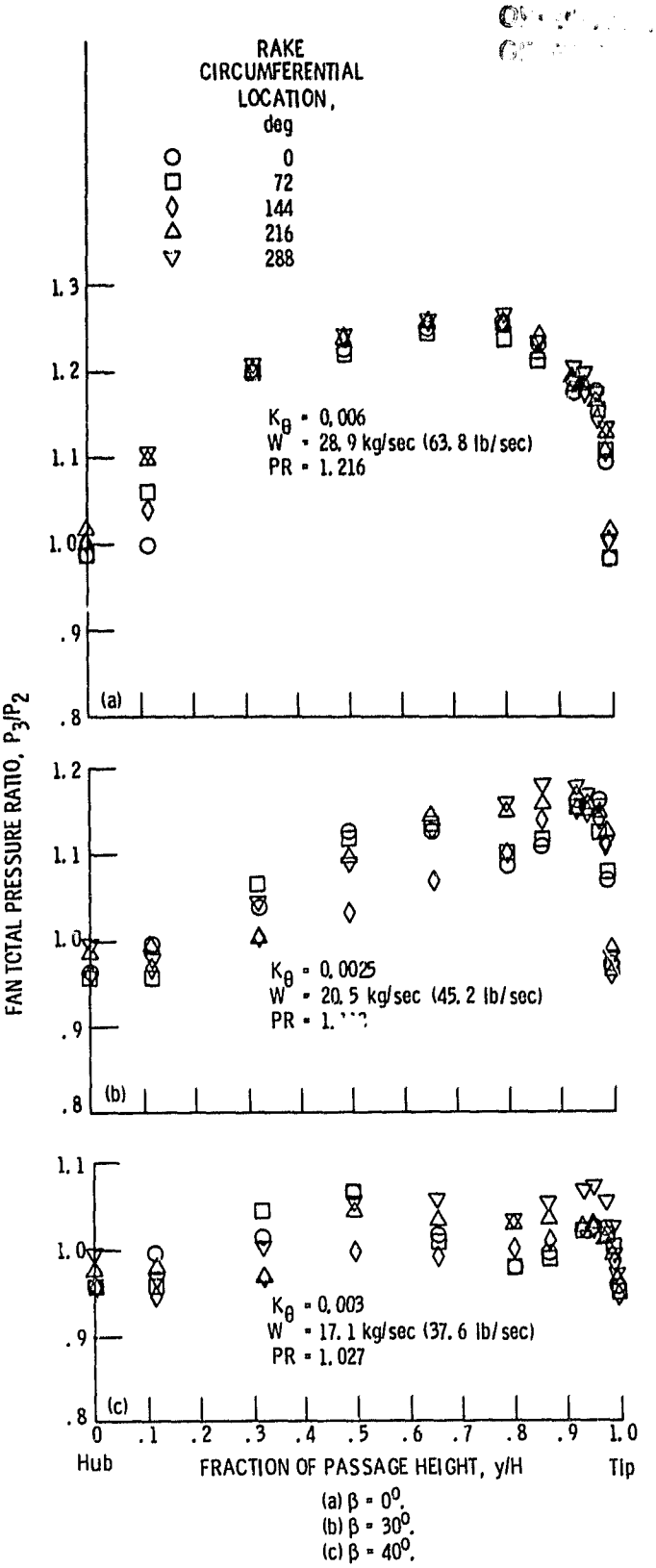

(a) $\beta = 0^0$.
(b) $\beta = 30^0$.
(c) $\beta = 40^0$.

Figure 9. - Stator exit total pressure profiles. Freestream velocity, 20.6 m/sec (40 knots); inlet angle-of-attack, 0^0; fan speed, 110% of design.

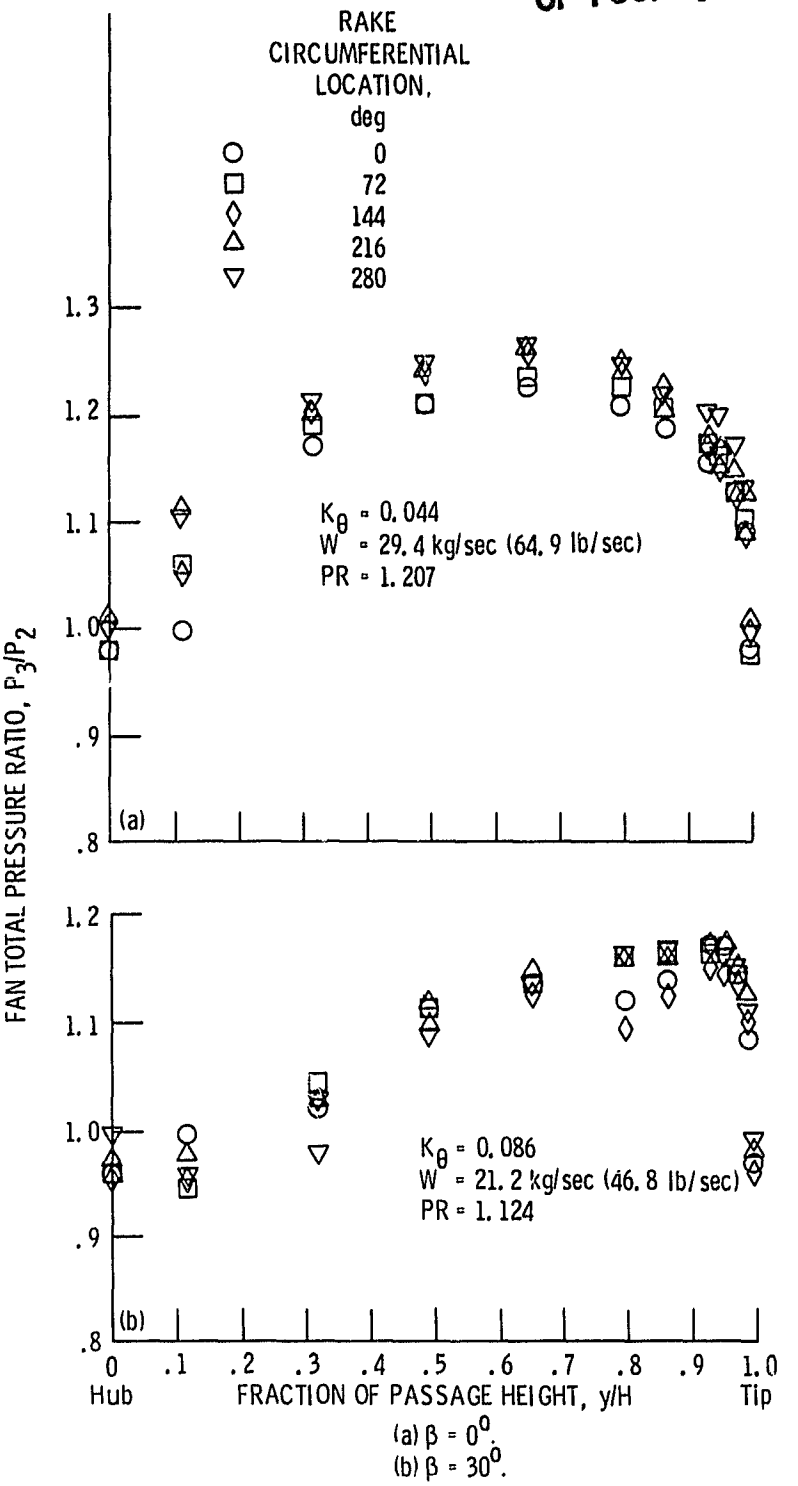

Figure 10. - Stator exit total pressure profiles. Freestream velocity 30.9 m/sec (60 knots); inlet angle-of-attack, 90^0; fan speed, 110% of design.

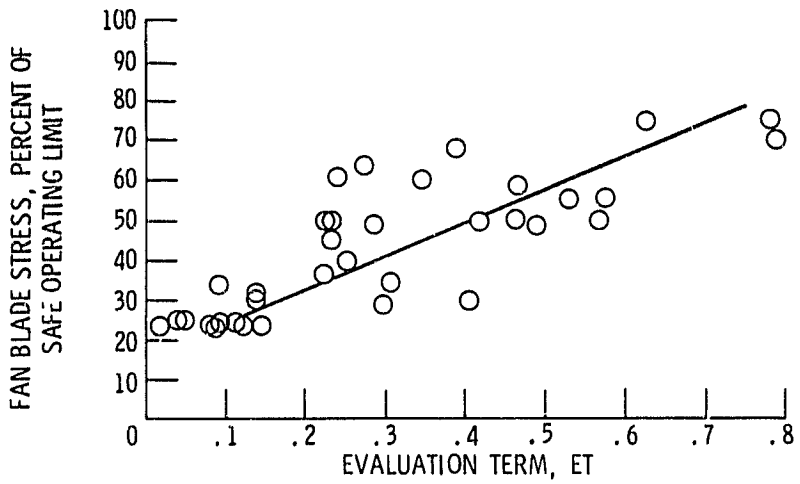

Figure 11. - Fan blade stress as a function of evaluation term.

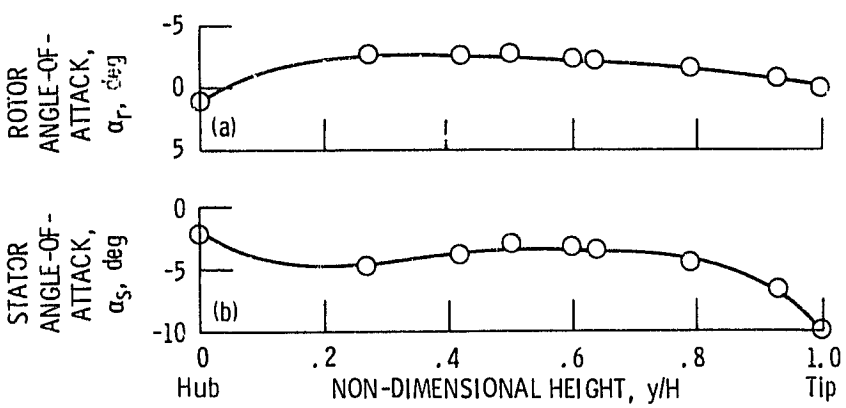

(a) Rotor.
(b) Stator.

Figure 12. - Calculated rotor and stator angle-of-attack as a function of radius. VIGV deflection angle, 0^0; free-stream velocity, 20.6 m/s (40 knots); fan speed, 110% of design; inlet angle-of-attack, 90^0.

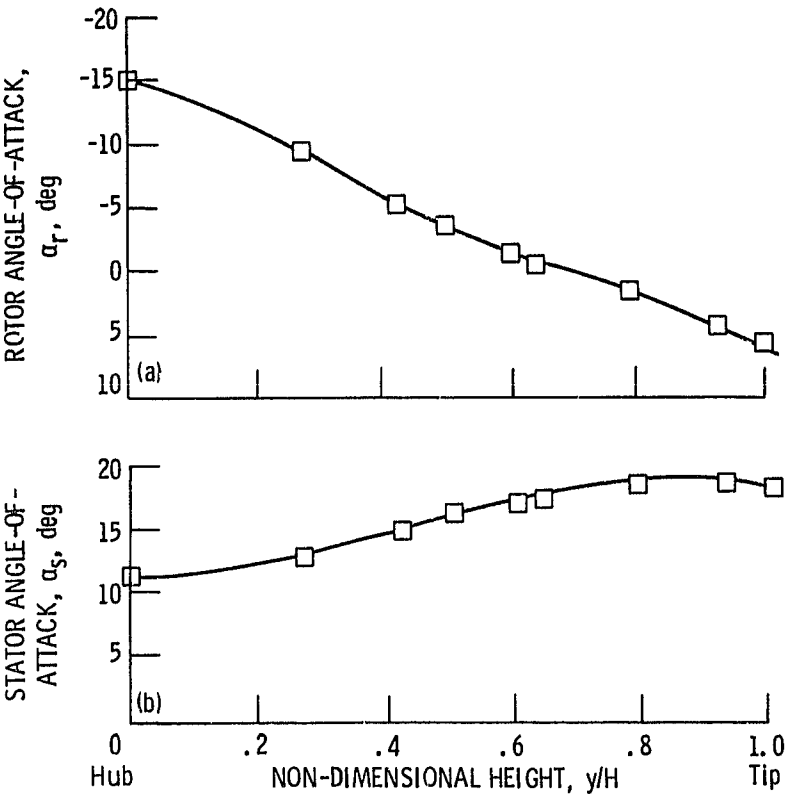

(a) Rotor.
(b) Stator

Figure 13. - Calculated rotor and stator angle-of-attack as a function of radius VIGV deflection angle, 40°; free-stream velocity, 20.6 m/s (40 knots); fan speed, 110% of design; inlet angle-of-attack, 90°.

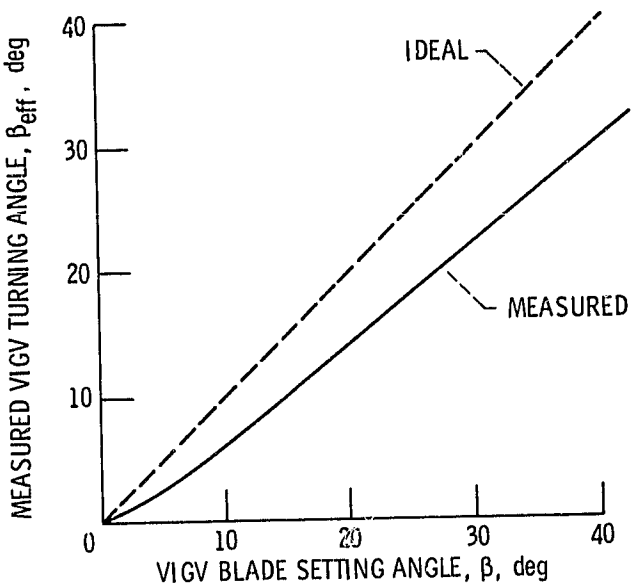

Figure 14. - Measured flow turning through the VIGV stage.